

Isotopic Composition of Solar Wind Calcium: First in situ Measurement by CELIAS/MTOF on board SOHO

R. Kallenbach¹, F. M. Ipavich², P. Bochsler³, S. Hefti³, P. Wurz³,
M. R. Aellig³, A. B. Galvin², J. Geiss¹, F. Gliem⁴, G. Gloeckler²,
H. Grünwaldt⁵, M. Hilchenbach⁵, D. Hovestadt⁶, and B. Klecker⁶

Received _____; accepted _____

To appear in the Astrophysical Journal as Letter

¹International Space Science Institute, Hallerstrasse 6, CH-3012 Bern, Switzerland,
reinald.kallenbach@issi.unibe.ch

²Dept. of Physics and Astronomy, University of Maryland, College Park, MD 20742,
USA

³Physikalisches Institut, University of Bern, CH-3012 Bern, Switzerland

⁴Institut für Datenverarbeitungsanlagen, Technische Universität, D-38106 Braunschweig,
Germany

⁵Max-Planck-Institut für Aeronomie, D-37189 Katlenburg-Lindau, Germany

⁶Max-Planck-Institut für Extraterrestrische Physik, D-85740 Garching, Germany

ABSTRACT

We present first results on the Ca isotopic abundances derived from the high resolution Mass Time-of-Flight (MTOF) spectrometer of the charge, element, and isotope analysis system (CELIAS) experiment on board the Solar and Heliospheric Observatory (SOHO). We obtain isotopic ratios $^{40}\text{Ca}/^{42}\text{Ca} = (128 \pm 47)$ and $^{40}\text{Ca}/^{44}\text{Ca} = (50 \pm 8)$, consistent with terrestrial values. This is the first in situ determination of the solar wind calcium isotopic composition and is important for studies of stellar modeling and solar system formation since the present-day solar Ca isotopic abundances are unchanged from their original isotopic composition in the solar nebula.

Subject headings: solar system: formation, Sun: abundances, Sun: solar wind

1. Introduction

The main motivation to study solar wind composition is to obtain information on the isotopic composition of elements in the Sun. This is important because the Sun constitutes 99.9% of solar system matter, and for most elements the solar composition could provide the most reliable information on the composition of the primordial solar nebula. Because nowhere in the Sun have temperatures ever been high enough to alter isotopic abundances of heavy elements by nuclear reactions, solar Ca is thought to reflect the original isotopic composition in the solar nebula. Yet, most of what is known of solar isotopic abundances is inferred from terrestrial and from meteoritic abundances with a few exceptions: recently, the isotopic composition of solar wind magnesium, the first analysis of the isotopic abundances of a refractive element in solar matter measured in situ with the spacecraft borne mass spectrometer WIND/MASS, has been reported (Bochsler et al., 1995). The solar isotopic composition of the volatile noble gases helium and neon have been determined in situ with the Apollo foil experiments (Geiss et al., 1972). In situ measurements with CELIAS/MTOF (Kallenbach et al., 1997) on board SOHO have confirmed that the solar neon isotopic composition differs significantly from the terrestrial and meteoritic abundances. Isotopic abundances also have been determined for several elements (C, N, O, He, Ne, Mg) in the higher energy (above 10 MeV/amu) solar energetic particles (Leske et al., 1996, Mason et al., 1994, Mewaldt et al., 1984, Selesnick et al., 1993). From similar measurements it has been possible to obtain reliable information on coronal elemental abundances including the abundance of calcium (Breneman and Stone 1985). However, the isotopic composition of solar energetic particles (SEP) may not be representative of the solar composition because fractionation processes occur during the particle acceleration and transport and these processes may vary from event to event. The far more fluent solar wind is the most authentic sample of the solar source composition. From recent theoretical models (e.g. Bodmer and Bochsler 1996) it is expected that the isotopic fractionation in the solar

wind flow due to differences in Coulomb drag depletes the heavier isotopes by at most a few percent. Therefore measurements of the solar wind isotopic abundances of the heavy element calcium together with previous measurements of magnesium abundances provide additional evidence that the solar isotopic composition of refractive elements agrees with terrestrial and meteoritic values.

2. Instrumentation

EDITOR: PLACE FIGURE 1 HERE.

The MTOF sensor (Figure 1) of CELIAS (Charge, Element, and Isotope Analysis System) on board the SOHO (Solar and Heliospheric Observatory) spacecraft is an isochronous time-of-flight mass spectrometer (Hovestadt et al., 1995) with a resolution $M/\Delta M$ of better than 100. This provides the possibility of resolving the different isotopes of almost all solar wind elements in the range from 3 to 60 atomic mass units (amu). The instrument detects ions at solar wind bulk velocities of 300 to 1000 km/s, corresponding to energies of about 0.3 to 3 keV/amu. Details on the principle of operation, the calibration of the instrument functions, and the format of the data transferred by the telemetry can be found in the initial publication on CELIAS/MTOF isotope abundance measurements of solar wind neon (Kallenbach et al., 1997). Here we only briefly describe the instrument characteristics which are necessary to understand the quantitative evaluation of time-of-flight (TOF) spectra.

Highly charged solar wind ions enter the instrument (Figure 1) through the WAVE (Wide Angle Variable Energy) entrance system that has an energy-per-charge (E/q) acceptance bandwidth of about half a decade, and a conic field of view of $\pm 25^\circ$ width (Hovestadt et al., 1995). All calcium isotopes have approximately the same bulk velocity, the same charge state, and the same width of the drifting maxwellian velocity distribution

so that the heavier isotopes have a higher center E/q . The strongest instrumental fractionation occurs when the center E/q of either isotope coincides with one of the edges of the E/q -acceptance of the WAVE. The acceptance function including the ion optical effects of the postacceleration voltage to the time-of-flight section has been well analyzed in the calibration system for mass spectrometers (Steinacher et al., 1995, Kallenbach et al., 1997) of the University of Bern (UoB). Therefore the flight data can reliably be filtered with respect to the ion optical instrument discrimination for any element or isotope detected in the solar wind. A much weaker instrumental fractionation is due to the element specific detection efficiencies of the VMASS subsystem which is a V-shaped isochronous time-of-flight spectrometer (Hovestadt et al., 1995). The ratio of the Double Coincidence Rate over the Front Secondary Electron Detection Assembly Rate has been measured as a function of ion energy per mass with a $^{40}\text{Ca}^{4+}$ beam of the MEFISTO laboratory at UoB (Marti 1997). The model functions reproduce the calibration data very well so that they can be applied to derive the differences in the detection efficiencies of the isotopes $^{40,42,44}\text{Ca}$ (Figure 2). With very good confidence the uncertainty of these detection efficiencies can be assumed to be lower than the statistical error evaluated (see Table 1).

EDITOR: PLACE FIGURE 2 HERE.

3. Data Analysis

EDITOR: PLACE FIGURE 3 HERE.

Figure 3 shows a spectrum where all pulse height analysis words of the full year 1996 have been collected in the mass range 39 to 45 amu. TOF channel contents have been put into bins six channels wide and the uncertainties of the data points have been estimated by the

linear-optimization algorithm of Rauch-Tung-Striebel (Gelb et al., 1974) where the filter width corresponds to half the TOF resolution of the instrument; this filter introduces a minor reduction of the peak resolution of 12%. This algorithm has been applied to improve the signal-to-noise ratio by a factor of four so that $^{42}\text{Ca}^+$ and $^{44}\text{Ca}^+$ can be identified with high significance. Note that most incident ions leave the carbon foil as neutrals or singly charged. The $^{40}\text{Ca}^+$ distribution is asymmetrically broadened. It exhibits a different shape than $^{20}\text{Ne}^+$ (Kallenbach et al., 1997) for one main reason: singly charged calcium has generally much higher E/q inside the VMAS than singly charged neon so that calcium follows a longer trajectory in the field free region above the ion stop microchannel plate (IMCP) detector (Hovestadt et al., 1995). Longer trajectories in the field-free region correspond to longer times of flight. This leads to the tails of higher channels in the TOF distribution of all the mass peaks in Figure 3. As in the case of $^{20,21,22}\text{Ne}^+$ (Kallenbach et al., 1997) the electronic ringing peaks are visible at about 30 TOF channels to the left of the $^{40,42,44}\text{Ca}^+$ signatures; they arise from reflected start signals. The TOF counts have been weighted by the detection efficiencies for the different calcium isotopes within the window of $\pm 15\%$ instrument fractionation between $^{44}\text{Ca}^+$ and $^{40}\text{Ca}^+$. All three detectable calcium peaks, $^{40}\text{Ca}^+$, $^{42}\text{Ca}^+$, and $^{44}\text{Ca}^+$, are described by the same model function with identical asymmetric shape. Also, the marginally detectable or non-detectable peaks $^{39,41}\text{K}^+$ and $^{43}\text{Ca}^+$ are included into the fit function, assuming terrestrial isotopic abundances:

$$\begin{aligned}
 F(t) = & \sum_{i=39}^{44} A_i \times \left(\exp\left[-\frac{(t-p_i)^2}{2s^2}\right] \right. \\
 & \left. + \sum_{j=1}^5 \frac{b_j}{1 + \frac{(t-p_i-jl)^2}{w^2}} \right. \\
 & \left. + c \times \exp\left[-\frac{(t-p_i+r)^2}{2u^2}\right] \right).
 \end{aligned}
 \tag{1}$$

t is the time-of-flight channel number and the free fit parameters are $A_{40,42,44}$ representing the amplitudes of the $^{40,42,44}\text{Ca}^+$ peaks, p_{40} the main Gaussian peak position of $^{40}\text{Ca}^+$, l the shift of the Lorentzians describing the asymmetry against the main Gaussians for all three peaks of $^{40,42,44}\text{Ca}^+$, r the shift of the ringing peaks against the main Gaussians, the b_j the relative amplitudes of the shifted Lorentzians compared to the main Gaussians, c the relative amplitude of the ringing peaks, s the width of the main Gaussian peaks, w the width of the Lorentzian peaks, and u the width of the ringing peaks. The Gaussian peak positions $p_{39,41,42,43,44}$ of $^{39,41}\text{K}^+$ and $^{42,43,44}\text{Ca}^+$ are kept fixed at their calibrated TOF channels. The total amplitudes $A_{40,42,44}$, the widths w and u , and the relative amplitudes b_j give the abundances for $^{40,42,44}\text{Ca}^+$. This analysis has been done twice assuming that the solar wind calcium is either tenfold or elevenfold charged.

EDITOR: PLACE TABLE 1 HERE.

Table 1 lists the integrated counts for $^{40,42,44}\text{Ca}^+$ assuming tenfold charged solar wind calcium. This gives the count ratios $^{40}\text{Ca}^+ / ^{42}\text{Ca}^+ = (100 \pm 25)$ and $^{40}\text{Ca}^+ / ^{44}\text{Ca}^+ = (45 \pm 4)$. Analogously, assuming elevenfold charged solar wind calcium we find $^{40}\text{Ca}^+ / ^{42}\text{Ca}^+ = (141 \pm 36)$ and $^{40}\text{Ca}^+ / ^{44}\text{Ca}^+ = (53 \pm 4)$. We further correct these ratios for the effect of heavy elements such as Si and Fe having different mean velocities in the solar wind compared to the proton velocity v_H derived from the proton monitor data. For Ca the mean velocity can be estimated to be $1.027 \times v_H - 14.6$ km/s (Hefti 1997). This correction in the mean velocity and therefore in the mean E/q leads to the values $^{40}\text{Ca}^+ / ^{42}\text{Ca}^+ = (107 \pm 25)$ and $^{40}\text{Ca}^+ / ^{44}\text{Ca}^+ = (46 \pm 4)$ for tenfold charged solar wind calcium and $^{40}\text{Ca}^+ / ^{42}\text{Ca}^+ = (148 \pm 36)$ and $^{40}\text{Ca}^+ / ^{44}\text{Ca}^+ = (54 \pm 4)$ for elevenfold charged solar wind calcium. According to Aellig et al. 1998 and Kern 1997 the coronal freeze-in temperatures for the time period considered in this paper are such that the average solar wind calcium charge state should be somewhere between ten and eleven; the average number is approximately

10.5. Therefore the final values for the solar wind calcium isotopic abundance ratios are taken as the average of the two values derived for the two assumptions of tenfold and elevenfold calcium. The error of the mean value is chosen sufficiently large to be compatible with both assumptions. For all ratios an additional uncertainty of 4% is due to uncertainties in the absolute calibration of the instrument acceptance. This results in $^{40}\text{Ca}^+ / ^{42}\text{Ca}^+ = (128 \pm 47)$ and $^{40}\text{Ca}^+ / ^{44}\text{Ca}^+ = (50 \pm 8)$. More precise values can be determined, once the charge distribution of solar wind calcium is better known for the year 1996 with other instrumentation on board the SOHO spacecraft. The sensors WIND/MASS and CELIAS/CTOF will provide sufficient information to reevaluate the calcium data.

4. Results

Based on the assumption that the solar wind calcium charge state varies between ten and eleven as a long term average, we find that the isotopic abundance ratios of solar wind calcium are $^{40}\text{Ca} / ^{42}\text{Ca} = (128 \pm 47)$ and $^{40}\text{Ca} / ^{44}\text{Ca} = (50 \pm 8)$. Both ratios are consistent with the terrestrial ratios $^{40}\text{Ca} / ^{42}\text{Ca} = (151.04 \pm 0.02)$ and $^{40}\text{Ca} / ^{44}\text{Ca} = (47.153 \pm 0.003)$ (Russell et al., 1977). More precise values can be obtained once a time series during the year 1996 of the calcium charge states in the solar wind at the SOHO location is available.

5. Discussion

From astrophysical and geochemical considerations it can be concluded that the isotopic composition of photospheric Ca must be within small fractions of per mills identical to the terrestrial composition. The similarity of the solar wind results with the terrestrial values suggests the preliminary conclusion that isotopic fractionation within the solar wind plays a minor role. This is supported by the model calculations of Bodmer and Bochsler 1996 that

consider differences in the Coulomb drag for isotopes of various elements. Fractionation effects not larger than a few percent are expected for Ne and Mg. For the heavy element Ca even weaker isotopic fractionation has to be expected. Although there are as yet no detailed evaluations of a more extensive time series with calcium isotopic ratios to be determined in different solar wind regimes, we suggest that the Ca abundance discussed in this work is within a few percent of the true solar composition.

Table 2 shows a comparison between the terrestrial, solar and presolar grain calcium isotopic composition. There is no evidence for large variations in these isotopic compositions except for the case of the presolar X-grains that originate from supernovae explosions (Hoppe et al., 1996, Nittler et al., 1996). The large enrichment in ^{44}Ca in the X-grains is a consequence of the radioactive decay of ^{44}Ti in supernovae material.

EDITOR: PLACE TABLE 2 HERE.

This work was supported by the Swiss National Science Foundation, by the PRODEX program of ESA, by NASA grant NAG5-2754, and by DARA, Germany, with grants 50 OC 89056 and 50 OC 9605. The flight-spare unit of MTOF has been recalibrated with the electron cyclotron resonance ion source in the MEFISTO laboratory at the University of Bern and with the support of Adrian Marti and Reto Schletti.

Table 1. Fitted parameters of the model function (Equation 1) for the calcium PHA spectrum.

	A_i (10+) ^a	A_i (11+) ^b	p_i ^c	Total Counts (10+) ^a	Total Counts (11+) ^b
⁴⁰ Ca ⁺	9756 ± 42	9600 ± 41	3053.1	58289 ± 251	57357 ± 245
⁴² Ca ⁺	98 ± 25	68 ± 17	3128.4	585 ± 149	406 ± 102
⁴³ Ca ⁺	14 ± 14	11 ± 11	3165.5	84 ± 84	66 ± 66
⁴⁴ Ca ⁺	218 ± 18	183 ± 15	3203.9	1302 ± 108	1093 ± 90
³⁹ K ⁺	148 ± 14	103 ± 12	3014.6	884 ± 84	615 ± 72
⁴¹ K ⁺	11 ± 11	7 ± 7	3091.0	64 ± 64	45 ± 45

^aData reduction based on the assumption of tenfold charged solar wind calcium.

^bData reduction based on the assumption of elevenfold charged solar wind calcium.

^cFixed calibrated relative peak positions with fitted offset to match spectrum of flight data.

Note. — The 1σ -errors of the amplitudes are determined with the method of maximum likelihood. The parameters that are equal for all isotopes and for both assumptions of ten- and elevenfold charged solar wind calcium have been fitted as $s = 9.222$, $b_1 = 0.023$, $b_2 = 0.009$, $b_3 = 0.047$, $b_4 = 0.178$, $b_5 = 0.117$, $l = 9.454$, and $w = 10.146$. The values for the ringing peaks have been taken from the neon evaluations and kept fixed: $c = 0.035$, $r = 31.66$, and $u = 5.71$.

Table 2. Results from measurements of the terrestrial, solar, and presolar calcium isotopic composition

$^{40}\text{Ca}/^{44}\text{Ca}$	$^{40}\text{Ca}/^{42}\text{Ca}$	Source	Reference
47.153 ± 0.003	151.04 ± 0.02	terrestrial	Russell et al., 1977
45.1 ± 0.8	147 ± 2	average of presolar grains	Amari et al., 1996
2.3 ± 0.2	...	presolar X-grain	Hoppe et al., 1996
50 ± 8	128 ± 47	solar wind (SOHO/CELIAS)	this work

REFERENCES

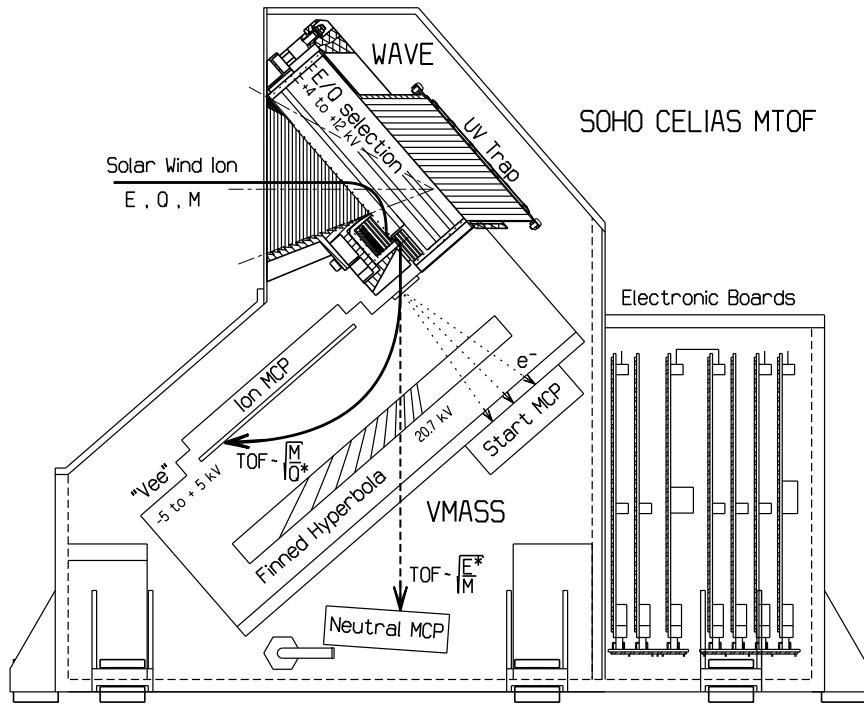
- Aellig, M., et al. 1998, submitted to J. Geophys. Res.
- Amari, S., Zinner, E., Lewis, R. S. 1996, Lunar Planet. Sci., 27, 23
- Breneman, H. H., and Stone, E. C. 1985, Astrophys. J., 299, L57
- Bochsler, P., Gonin, M., Sheldon, R. B., Zurbuchen, T., Gloeckler, G., Hamilton, D. C., Collier, M. R., and Hovestadt, D. 1995, Proc. 8th Int. Solar Wind Conf., D. Winterhalter, J. T. Gosling, S. R. Habbal, W. S. Kurth, M. Neugebauer, Woodbury:AIP Press, 1995, 199
- Bodmer, R., and Bochsler, P., paper presented at meeting, Eur. Geophys. Soc., The Hague, Netherlands, 1996
- Geiss, J., Bühler, F., Cerutti, H., Eberhardt, P., and Filleux, C. 1972, Apollo 16 Preliminary Scientific Report, NASA Spec. Publ., SP-315, 14.1
- Gelb, A., Kasper, J. F., Nash, R. A., Price, C. F., and Sutherland, A. A. 1974, Applied Optimal Estimation, A. Gelb, Cambridge:MIT Press, 1974.
- Gonin, M., Kallenbach, R., Bochsler, P., and Bürgi, A. 1995, Nucl. Instrum. Methods Phys. Res., B101, 313
- Hefti, S. 1997, PhD thesis, University of Bern, Switzerland
- Hoppe, P., Strebel, R., Eberhardt, P., Amari, S., and Lewis, R. S. 1996, Science, 272, 1314
- Hovestadt, D., et al. 1995, Solar Physics, 162, 441
- Kallenbach, R., et al. 1997, J. Geophys. Res., 102, 26895
- Kern, O. 1997, private communication, University of Bern, Switzerland

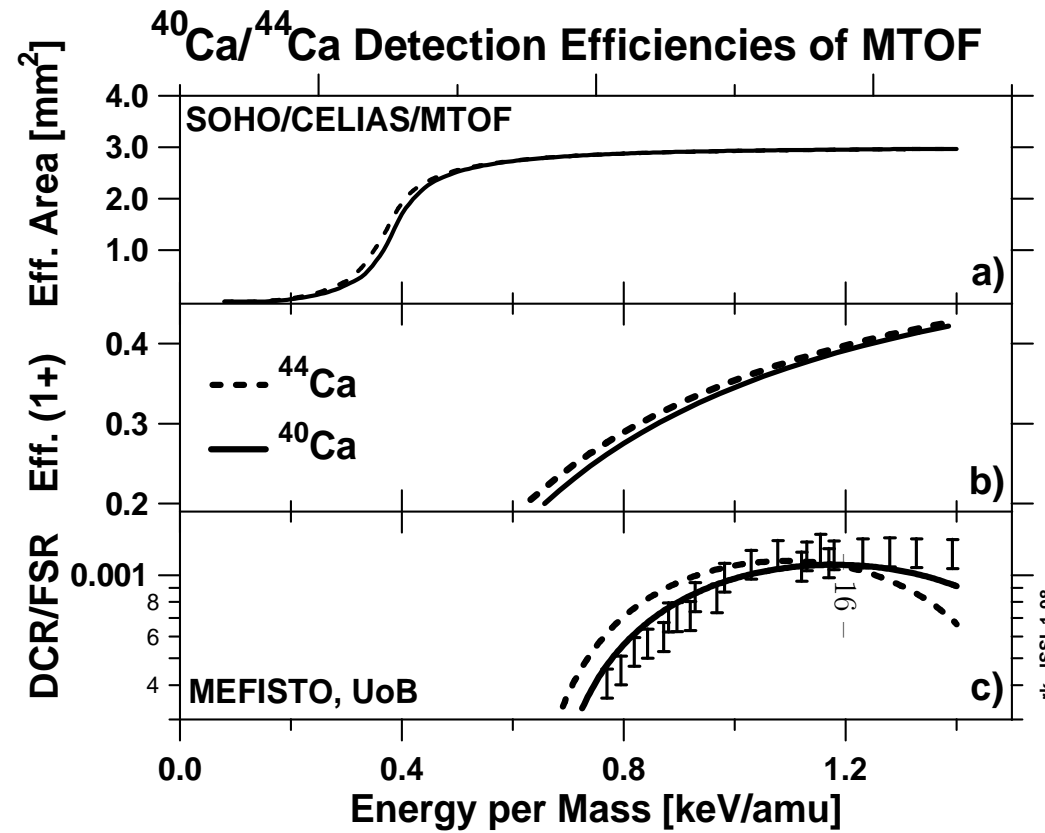
- Leske, R. A., Mewaldt, R. A., Cummings, A. C., Cummings, J. R., Stone, E. C., and von
Rosenvinge, T. T. 1996, *Space Sci. Rev.*, 78, 149
- Marti, A. 1997, PhD thesis, University of Bern, Switzerland
- Mason, G. M., Mazur, J. E., and Hamilton, D. C. 1994, *Astrophys. J.*, 425, 843
- Mewaldt, R. A., Spalding, J. D., and Stone, E. C. 1984, *Astrophys. J.*, 280, 892
- Nittler, L. R., Amari, S., Zinner, E., Woosley, S. E., and Lewis, R. S. 1996, *Astrophys. J.*,
462, L31
- Russell, W. A., Papanastassiou, D. A., Tombrello, T. A., and Epstein, S. 1977, *Proc. Lunar
Sci. Conf. 8th*, 3791
- Selesnick, R. S., Cummings, A. C., Cummings, J. R., Leske, R. A., Mewaldt, R. A., Stone,
E. C., and von Rosevinge, T. T. 1993, *Astrophys. J.*, 418, L45
- Steinacher, M., Jost, F., and Schwab, U. 1995, *Rev. Sci. Instrum.*, 66, 4180
- Zurbuchen, T., Bochsler, P., and Scholze, F. 1995, *Opt. Eng.*, 34, 1303

Fig. 1.— Schematic view of the SOHO/CELIAS/MTOF sensor.

Fig. 2.— a) Front Secondary Electron Detection Assembly Rate (FSR) model functions versus energy per mass in units of mm^2 representing the effective detection area of the CELIAS/MTOF sensor at optimum orientation and energy-per-charge acceptance. b) Illustrates the probability that the ^{40}Ca and ^{44}Ca isotopes leave the foil singly ionized. Most particles leave the carbon foil at the entrance of the isochronous time-of-flight spectrometer VMAS as neutrals or singly charged. c) Double Coincidence Rate (DCR) of $^{40}\text{Ca}^+$ and $^{44}\text{Ca}^+$ over FSR versus ion energy-per-mass ratio: the calibration data from the MEFISTO ion source at UoB (Marti 1997) are described by a model that includes charge exchange processes, energy loss and straggling, including its corresponding angular scattering in the carbon foil, ion optics, and the stop detector efficiency. At the low energies $^{44}\text{Ca}^+$ has a higher chance to be detected than $^{40}\text{Ca}^+$ because the heavier isotope suffers less angular straggling, whereas at the higher energies $^{44}\text{Ca}^+$ has a higher risk to overshoot the ion stop micro channel plate (IMCP) or to hit the hyperbola deflection electrode than $^{40}\text{Ca}^+$ because the heavier particle suffers less energy loss.

Fig. 3.— Time-of-flight spectrum derived from the pulse height analysis words of the full year 1996 filtered with respect to instrument fractionation with a window of $\pm 15\%$. A background of 1500 counts has been subtracted in the diagram but has been included in the error estimation with the linear-optimization algorithm of Rauch-Tung-Striebel (Gelb et al., 1974). The solid line represents the fitted model function of the TOF response. The analysis shown here assumes that the solar wind calcium always entered the instrument tenfold charged. The same analysis has been redone assuming elevenfold charged solar wind calcium (see text).





Calcium PHA Data 1996

(selected for samples < 15% instrument fractionation)

